Impact of Optical System Size on Robustness in Laser Speckle Authentication

Naoki Fujieda [1] Kazuya Kitano [1] Takuya Funatomi [1]
Rui Ishiyama [1,2] Yasuhiro Mukaigawa [1]

[1] NAIST
Ikoma, Nara 630–0192, Japan

[2] NEC Corporation
Kawasaki, Kanagawa 211–8666, Japan

Abstract

Laser Speckle Authentication (LSA) has been widely studied, yet the impact of the optical system size on its robustness against object misalignment remains under-explored. To clarify this, we evaluated the effects of perpendicular and parallel misalignments using six optical systems combining lens-based and lensless configurations. Our findings reveal that lens-based systems exhibit superior robustness against misalignment although they require a larger system size. This research provides insights for developing compact, robust authentication systems under practical size constraints.

1 Introduction

In modern manufacturing, confirming the authenticity of products and preventing the distribution of counterfeit goods is important. Traditionally, authentication using identifiers such as barcodes and QR-codes has been performed; however, these methods carry risks of tampering and replication. Consequently, artificial metrics technologies, which utilize the physical characteristics generated during the manufacturing process, have attracted attention [1–3]. One of them is a Laser Speckle Authentication (LSA) which identifies and authenticates individual objects by using the speckle pattern observed when laser light is irradiated onto the object surface. While it offers high identification accuracy without label attachment, the speckle pattern is sensitive to imaging conditions and object misalignment, which poses challenges regarding practical robustness. Although several studies on LSA have been conducted [4–7], discussion is still insufficient regarding the influence of the presence or absence of a lens, as well as the optical system size, on the robustness against object misalignment.

In this study, aiming to clarify the influence of the optical system size on the robustness of LSA, we evaluated the changes in speckle patterns when an object was moved in both perpendicular and parallel translations relative to the optical axis using six types of optical systems combining lens-based and lensless configurations. As a result, it was confirmed that lens-based optical systems exhibit high robustness against object misalignment at the expense of an increased system size, and that translation in the perpendicular direction relative to the optical axis has minimal impact with respect to the distance between the sensor and the object. The findings of this study provide guidelines for the design of optical systems toward the practical implementation of LSA.

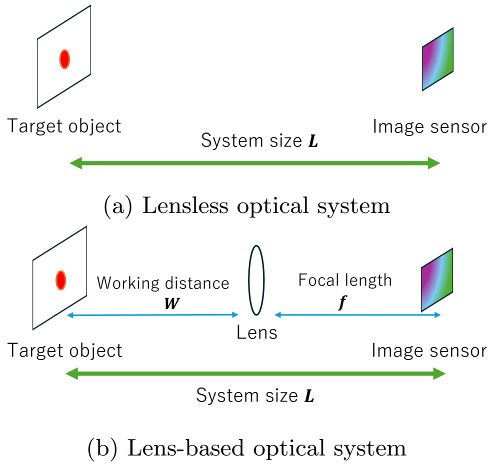

Figure 1: Definition of the optical system size

2 Design of Optical Systems for LSA

Laser speckles are random granular patterns that occur when coherent light irradiated a rough surface, and their size depends on the parameters of the optical system [8]. This section examines the relationship between speckle size, image sensor sampling, and system dimensions in lensless and lens-based optical systems.

In its most elementary form, an LSA setup requires only a coherent laser source, the target object to be authenticated, and an image sensor (Fig. 1(a)). In this study, the system size L is defined as the distance from the target object to the image plane in a lensless optical system(Fig. 1(a)), and as the sum of the working

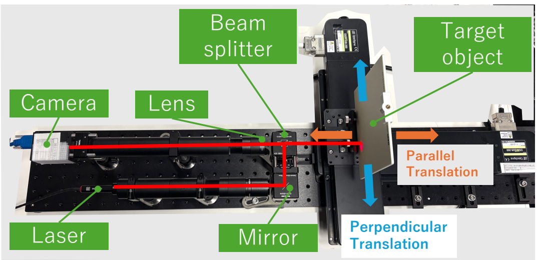

Figure 2: Hardware implementation

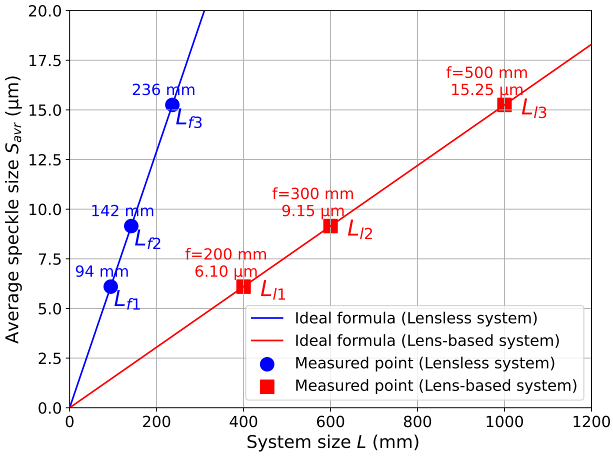

Figure 3: Relationship between system size and average speckle size

distance W and the focal length f in a lens-based optical system (Fig. 1(b)). Additionally, treating the lens as a Fourier transform lens, we place the target object at the focal distance.

The maximum number of objects that can be authenticated depends on speckle pattern coarseness. The minimum speckle size S_{min} is given by

$$S_{\text{min}} = \begin{cases} \frac{\lambda L}{\alpha} & \text{(Lensless optical system)} \\ \frac{\lambda}{\beta} & \text{(Lens-based optical system)} \end{cases} \quad (1)$$

where λ is the laser wavelength, L is the distance from the target object to the image plane, α is the beam diameter, and β is the divergence angle from the pupil plane. The average speckle size, considering the Rayleigh criterion, is

$$S_{\text{avr}} = 1.22\ S_{\text{min}}. \quad (2)$$

Based on the sampling theorem, the relationship between the speckle size observed on the image plane and the pixel size L_{px} of the image sensor is given by

$$S_{\text{avr}} \geq 2\ L_{\text{px}}. \quad (3)$$

3 Hardware Implementation

We target an optical system in which a laser beam is irradiated onto the target object and the image sensor is parallel to the object plane as shown in Fig. 2. The light source is a semiconductor laser (THORLABS, PL202), and a beam expander is used to adjust the beam diameter to 12mm. A coaxial system is constructed with a mirror and a beam splitter (THORLABS, CCM1-E02/M and CCM1-PBS251/M). A camera (FLIR, GS3-U3-28S5M-C; pixel size: 4.54µm, resolution: 1,920×1,440) and a screen (THORLABS, EDU-VS1) as the target object are used.

In this study, we evaluated six optical configurations. These consisted of three lensless systems (L_{f1} to L_{f3}) and three lens-based systems (L_{l1} to L_{l3}). Each configuration was designed so that its average speckle size would be equal to, larger than, or smaller than the value given by Eq. 3. The lens-based systems L_{l1} to L_{l3} employed plano-convex lenses with a diameter of 25.4mm and focal lengths f=200, 300, 500mm (THORLABS, LB1945, LB1779, LB1869), corresponding to ideal average speckle sizes of 6.10, 9.15, 15.25µm, respectively. Because the number of objects that can be authenticated is limited by speckle coarseness, we configured the lensless systems to match the average speckle size of lens-based systems. Fig. 3 shows that obtaining the same speckle size requires a larger overall system length in the lens-based case. This difference arises because, according to Eqs. (1) and (2), speckle size in lensless systems depends on beam diameter and propagation distance, whereas in lens-based systems it is governed by lens aperture. The propagation distance of the lensless setups was therefore adjusted to compensate for the limited choice of commercial lenses.

4 Experiments and Evaluation

In this experiment, the laser beam was irradiated onto two distinct points on the screen, and different speckle patterns were observed. These two points were spaced sufficiently apart such that, even for the same product, completely different speckle patterns could be observed depending on the position of irradiation. Therefore, they are regarded as two different objects, referred to as object A and B, respectively.

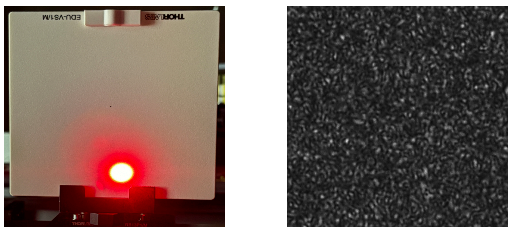

Figure 4: Screen as a target object and the speckle

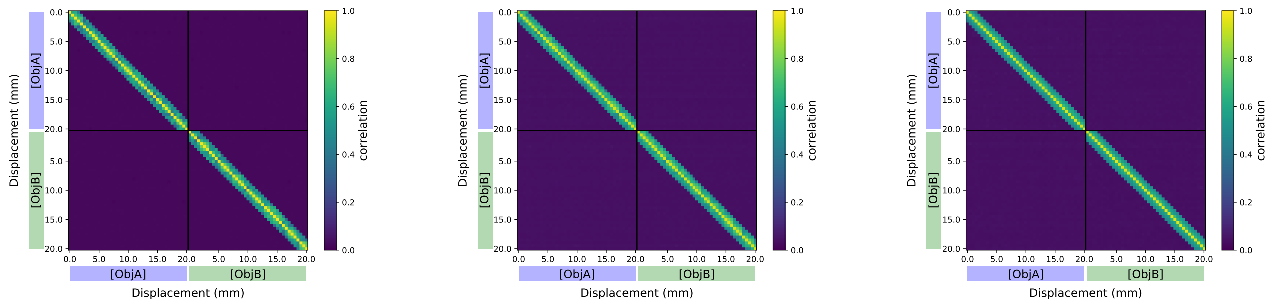

(a) Lensless Optical System(L_{f1}) (b) Lensless Optical System(L_{f2}) (c) Lensless Optical System(L_{f3})

Figure 5: Lensless — Correlation Matrix under Perpendicular Displacement

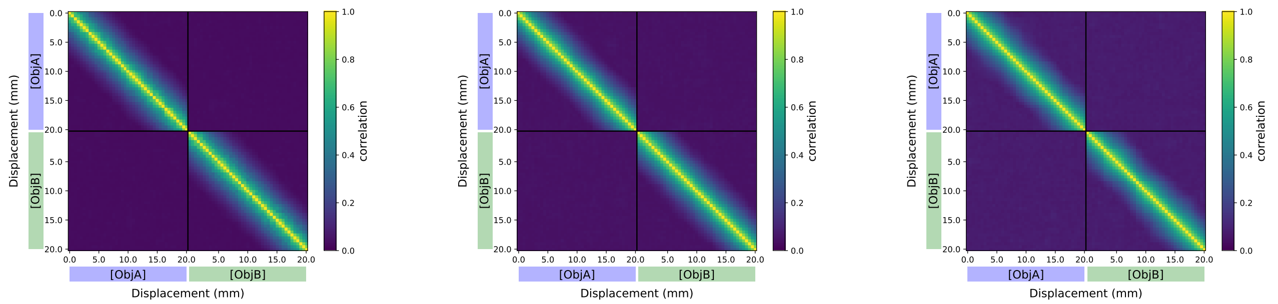

(a) Lens-based Optical System(L_{l1}) (b) Lens-based Optical System(L_{l2}) (c) Lens-based Optical System(L_{l3})

Figure 6: Lens-based — Correlation Matrix under Perpendicular Displacement

The screen was translated relative to the optical axis in both perpendicular and parallel directions in steps of 0.5mm over a range of ±10mm to evaluate the robustness of the authentication. As a result, 21 speckle images were acquired for each object and 42 images in total. For each speckle image, a query image was generated by cropping a 1,024×1,024 pixels from the center of the image. In addition, template images were sequentially generated by cropping 256×256 pixels. For all pairs of template and query images from the 42 speckle images, we computed the normalized cross-correlation using template matching. An example speckle image from system L_{f2} is shown in Fig. 4.

The results are visualized as a four-panel correlation matrix (Fig. 5–8) showing template–observed image correlations for two objects. The top-left panel shows correlations between object-A's template and its observed images, while the top-right shows correlations with object-B's observed images. The bottom-left panel shows correlations between object-B's template and object-A's observed images, while the bottom-right shows correlations with its own observed images.

The distribution of correlation values was evaluated between images of the same object and between images of different objects. The correlation values were evaluated on a scale from 0.0 to 1.0. If the distributions for the same and different objects are completely separated, setting a threshold allows for error-free individual identification. Furthermore, wide diagonal bands in the correlation matrix indicate high robustness to misalignment, whereas narrow diagonal bands indicate low robustness.

4.1 Robustness against Perpendicular Translation

The results of translating the screen in the perpendicular direction for each optical system are shown in Fig. 5 and Fig. 6.

The optical systems L_{f1} to L_{f3} exhibited similar robustness, consistently around $3.5mm$. This suggests that, in lensless optical systems, the system size L has little effect on robustness against perpendicular translation. Similarly, all lens-based systems L_{l1} to L_{l3} demonstrated consistent robustness against perpendicular translation, independent of the system size L. However, compared to lensless optical systems, the lens-based systems demonstrated higher robustness, as identification was possible even with a displacement of approximately 10mm.

4.2 Robustness against Parallel Translation

For the lensless optical systems, the results obtained by translating the screen in the parallel direction are

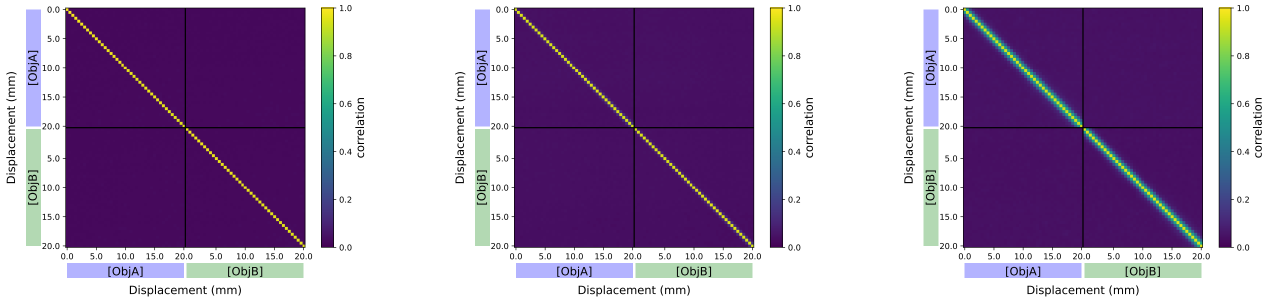

(a) Lensless Optical System(L_{f1}) (b) Lensless Optical System(L_{f2}) (c) Lensless Optical System(L_{f3})

Figure 7: Lensless — Correlation Matrix under Parallel Displacement

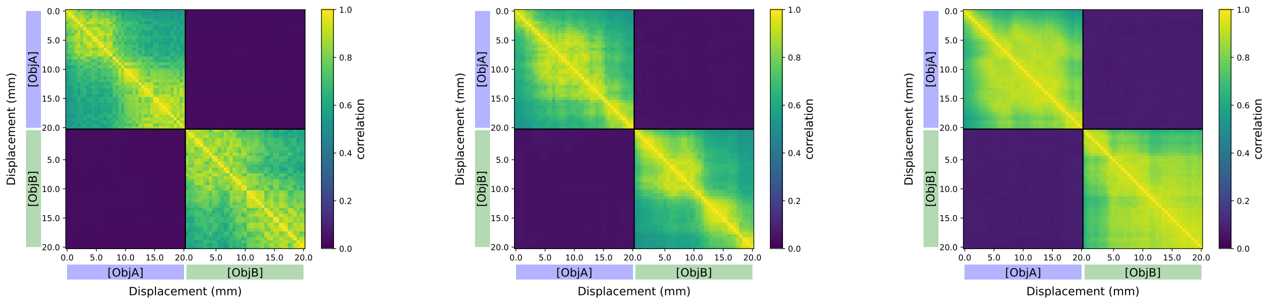

(a) Lens-based Optical System(L_{l1}) (b) Lens-based Optical System(L_{l2}) (c) Lens-based Optical System(L_{l3})

Figure 8: Lens-based — Correlation Matrix under Parallel Displacement

shown in Fig. 7. Unlike the case for perpendicular translation, in optical systems L_{f1} and L_{f2} the diagonal elements of the correlation matrix are very narrow, indicating low robustness. However, in optical system L_{f3}, a robustness of 2.5mm was observed, suggesting that increasing the system size can improve robustness. Overall, the lensless optical systems exhibit lower robustness against parallel translation compared to perpendicular translation.

Figure 8 shows the results for the lens-based optical systems. In all systems, high correlation values are observed in the upper left and lower right regions of the correlation matrix, indicating that the screen can be correctly identified even with a displacement of 20mm. Furthermore, the correlation values computed within the same object increase in the order $f_{l_1} < f_{l_2} < f_{l_3}$, demonstrating that increasing the system size and using a lens with a longer focal length enhances the stability.

5 Conclusion

In this study, the optimal optical system for LSA was analyzed from the viewpoints of system size and the robustness against object misalignment. It was shown that high robustness against object misalignment can be achieved by ensuring a sufficient system size and employing a lens-based optical system with a long focal length. Although there was no significant difference in the robustness against perpendicular translation between lens-based and lensless optical systems with respect to system size, the lens-based optical systems demonstrated higher robustness. Thus, when size is unconstrained and stable authentication is required, a lens-based system is recommended.

While lensless optical systems can be made more compact when considering the same average speckle size, their robustness against object misalignment is lower than that of lens-based systems. However, lensless systems can also be a viable option in cases where system size is highly constrained and the misalignment is small. For example, a tolerance of approximately 2.5mm in the parallel direction and approximately 3.5mm in the perpendicular direction can be achieved when the system size L=236mm is allowed.

In this study, we used a template matching technique, further improvements in correlation algorithms and exploration of alternative matching techniques should enhance LSA's robustness and practical applicability. Moreover, this study only considered translational and axial misalignment, however rotational and tilt misalignment also impact robustness and should be analyzed and mitigated for practical applications.

References

[1] Guidelines for interoperable object identification and related authentication systems to deter counterfeiting and illicit trade. *ISO*, (ISO/DIS 22378), 12 2022.

[2] James Buchanan, Russell Cowburn, Ana-Vanessa Jausovec, Dorothee Petit, Peter Seem, Gang Xiong, Del Atkinson, Kate Fenton, Dan Allwood, and Matthew Bryan. Forgery: 'fingerprinting' documents and packaging. *Nature*, 436:475, 08 2005.

[3] Y. Blau, O. Bar-On, Y. Hanein, A. Boag, and J. Scheuer. Meta-hologram-based authentication scheme employing a speckle pattern fingerprint. *Opt. Express*, 28(6):8924–8936, Mar 2020.

[4] F. van Beijnum, E. G. van Putten, K. L. van der Molen, and A. P. Mosk. Recognition of paper samples by correlation of their speckle patterns, 2006. arXiv preprint arXiv:physics/0610089.

[5] Manabu Yamakoshi, Xiaoying Rong, and Tsutomu Matsumoto. An artifact-metrics which utilizes laser speckle patterns for plastic id card surface. In Liang-Chy Chien, editor, *Emerging Liquid Crystal Technologies V*, volume 7618, page 76180B. SPIE, February 2010.

[6] Wiwi Samsul, Henri P. Uranus, and M.D. Birowosuto. Recognizing document's originality by laser surface authentication. In *2010 Second International Conference on Advances in Computing, Control, and Telecommunication Technologies*, pages 37–40, 2010.

[7] Wiwi Samsul, Henri Uranus, and Muhammad Danang Birowosuto. Static laser surface authentication with low-cost microscope: Tolerances on spatial and angular disturbance. *Journal of Optics*, 44:1–8, 05 2015.

[8] Pavel Horváth, M. Hrabovsky, and Petr Šmíd. Full theory of speckle displacement and decorrelation in the image field by wave and geometrical descriptions and its application in mechanics. *Journal of Modern Optics*, 51:725–742, 03 2004.